

## Targeting cytokine-induced leukemic stem cell persistence in chronic myeloid leukemia by IKK2-inhibition

by Marlena Bütow, Fabio J. Testaquadra, Julian Baumeister, Tiago Maié, Nicolas Chatain, Timo Jaquet, Stefan Tillmann, Martina Crysandt, Ivan G. Costa, Tim H. Brümmendorf, and Mirle Schemionek

*Received: March 10, 2022.*

*Accepted: November 23, 2022.*

*Citation: Marlena Bütow, Fabio J. Testaquadra, Julian Baumeister, Tiago Maié, Nicolas Chatain, Timo Jaquet, Stefan Tillmann, Martina Crysandt, Ivan G. Costa, Tim H. Brümmendorf, and Mirle Schemionek. Targeting cytokine-induced leukemic stem cell persistence in chronic myeloid leukemia by IKK2-inhibition.*

*Haematologica. 2022 Dec 1. doi: 10.3324/haematol.2022.280922 [Epub ahead of print]*

### *Publisher's Disclaimer.*

*E-publishing ahead of print is increasingly important for the rapid dissemination of science. Haematologica is, therefore, E-publishing PDF files of an early version of manuscripts that have completed a regular peer review and have been accepted for publication. E-publishing of this PDF file has been approved by the authors. After having E-published Ahead of Print, manuscripts will then undergo technical and English editing, typesetting, proof correction and be presented for the authors' final approval; the final version of the manuscript will then appear in a regular issue of the journal. All legal disclaimers that apply to the journal also pertain to this production process.*

# Targeting cytokine-induced leukemic stem cell persistence in chronic myeloid leukemia by IKK2-inhibition

Marlena Bütow<sup>1,2</sup>, Fabio J. Testaquadra<sup>1,2</sup>, Julian Baumeister<sup>1,2</sup>, Tiago Maié<sup>3</sup>, Nicolas Chatain<sup>1,2</sup>, Timo Jaquet<sup>1,2</sup>, Stefan Tillmann<sup>1,2</sup>, Martina Crysandt<sup>1,2</sup>, Ivan G. Costa<sup>3</sup>, Tim H. Brümmendorf<sup>1,2</sup>, Mirle Schemionek<sup>1,2</sup>

<sup>1</sup>Department of Hematology, Oncology, Hemostaseology, and Stem Cell Transplantation, Faculty of Medicine, RWTH Aachen University, Aachen, Germany, <sup>2</sup>Center for Integrated Oncology Aachen Bonn Cologne Düsseldorf (CIO ABCD), Aachen, Germany, <sup>3</sup>Institute for Computational Genomics, Joint Research Center for Computational Biomedicine, RWTH Aachen University, Aachen, Germany

**Correspondence** Mirle Schemionek-Reinders, PhD, Department of Hematology, Oncology, Hemostaseology, and Stem Cell Transplantation, Faculty of Medicine, RWTH Aachen University, Aachen, Germany, Pauwelsstraße 30, 52074 Aachen, Germany, Center for Integrated Oncology Aachen Bonn Cologne Düsseldorf (CIO ABCD), Aachen, Germany.

E-Mail: [mschemionek@ukaachen.de](mailto:mschemionek@ukaachen.de)

## Acknowledgements

The authors thank Dr. Vignir Helgason and Dr. Eric Kalkman for providing KCL22 T315I cells, Julia Plum and Kristina Pannen for excellent technical assistance, and Dr. Jörg Eschweiler for providing healthy donor-derived cells. This work was supported by the IHC (immunohistochemistry) facility, a core facility of the Interdisciplinary Center for Clinical Research (IZKF) Aachen, within the Faculty of Medicine at RWTH Aachen University. Figures were created with BioRender.com.

## **Funding**

This work was supported by the Clinical Research Group entitled “Untangling and Targeting Mechanisms of Myelofibrosis in Myeloproliferative Neoplasms (MPN)” (CRU344) funded by the German Research Foundation (DFG) (SCHE 1938/3-1 [AOBJ 659838]), in the framework of the Research Training Group “Tumor-targeted Drug Delivery” grant 331065168 as well as by the START-Program of the Faculty of Medicine, RWTH Aachen (grant 691706).

## **Authorship contributions**

MB designed research, performed experiments, analyzed the data and wrote the manuscript. FJT and JB performed experiments and revised the manuscript. NC, TJ and ST assisted experimental work and revised the manuscript. IGC and TM reanalyzed publicly available expression data sets. MC contributed patient samples and clinical data. THB contributed research material and revised the manuscript. MS designed research, analyzed the data and revised the manuscript. Final approval of the manuscript was provided by all authors.

## **Competing interests**

The authors declare no conflict of interest.

## **Availability of data and materials**

[GSE40721] <https://www.ncbi.nlm.nih.gov/geo/query/acc.cgi?acc=gse40721>

[GSE47927] <https://www.ncbi.nlm.nih.gov/geo/query/acc.cgi?acc=gse47927>

## **Data-sharing statement**

All technical information pertaining to the experimentation performed is available on request.

Chronic myeloid leukemia (CML) is a clonal myeloproliferative disorder, arising from a hematopoietic stem cell (HSC) that acquires the chromosomal translocation t(9;22), resulting in the BCR-ABL oncoprotein. While BCR-ABL-targeting tyrosine kinase inhibitors (TKIs) eliminate the majority of CML-cells, the most primitive disease-initiating leukemic stem cells (LSCs) are frequently spared. CML development is accompanied by increasing levels of inflammatory cytokines, such as IL-1 $\alpha$ , IL-1 $\beta$ , IL-6, or TNF. Correspondingly, LSCs are characterized by a TKI-persisting, inflammatory cytokine-response pattern that was observed even during prolonged therapy.<sup>1</sup> Our preliminary work confirmed that TNF-signaling is active in murine CML stem cells and TNF-targeted antibody treatment enhanced therapeutic efficiency of TKI-treatment.<sup>2</sup> Moreover IKK-dependent activation of NF- $\kappa$ B has been shown to contribute to BCR-ABL-induced myeloid and lymphoid leukemogenesis.<sup>3,4</sup> In CML stem and progenitor cells, an autocrine TNF-loop and NF- $\kappa$ B signaling were found to persist during TKI-treatment *in vitro*.<sup>5</sup> NF- $\kappa$ B serves as a central inflammatory hub as several cytokines induce IKK-dependent phosphorylation at serine 32/36 and subsequent degradation of I $\kappa$ B $\alpha$ , which releases the NF- $\kappa$ B complex, allowing its activation by phosphorylation at serine 536 and transport to the nucleus.<sup>6</sup> Thereby, NF- $\kappa$ B induces transcription of target genes such as several cytokines or the NF- $\kappa$ B signaling molecules themselves.<sup>7</sup> Here we confirmed TKI-persistent TNF-induced NF- $\kappa$ B signaling in CML mice and human cells. As TNF can induce pro-proliferative signaling via NF- $\kappa$ B but also pro-apoptotic cascades via RIPK1 induced CASP8 activation, we here aimed to specifically inhibit the pro-proliferative activity by targeting IKK2. Therefore, we performed pharmacologic IKK2-inhibition, using the small molecule IKK2-inhibitor LY2409881 (LY), previously observed as well tolerable in pre-clinical application.<sup>8</sup> Combined BCR-ABL/IKK2-targeting blocked malignant NF- $\kappa$ B signaling and enhanced apoptosis in TKI-sensitive but also -resistant cells. *In vivo*, NF- $\kappa$ B-mediated TNF-activity was elevated despite nilotinib (NIL) treatment. IKK2-targeting severely reduced LSCs, which was further reflected by preventing disease onset upon secondary transplantation. As TNF-induced NF- $\kappa$ B-signaling was evident in chronic phase (CP) but likewise blast crisis (BC)-CML, IKK2-targeting affected the clonogenic potential in both disease stages. Finally, in

CP-CML CD34<sup>+</sup> cells, combined BCR-ABL/IKK2-inhibition significantly induced apoptosis, also in quiescent LSCs showing that this approach enables the eradication of the TKI-persisting malignant stem cell population in CML.

Aiming to get insight into the role of malignant TNF-signaling in CML, we started to compare BCR-ABL-positive vs –negative cell lines. We observed significant upregulation of TNF-signaling in 32D BCR-ABL vs. empty vector control cells, as represented by increased expression of relevant TNF-targets in BCR-ABL positive cells (*I $\kappa$ B $\alpha$* , fold change (fc): 1.9; *Nf- $\kappa$ B*, fc: 2.2, *A20*, fc: 6.5, *Online Supplementary Figure S1A*). To mimic the malignant inflammatory niche, TNF was subsequently added to both cell types at a physiological concentration and this still resulted in increased TNF-target gene expression in BCR-ABL vs. control cells (*I $\kappa$ B $\alpha$* , fc: 1.7; *Nf- $\kappa$ B*, fc: 3, *A20*, fc: 3.4). Notably, this upregulation of TNF-signaling persisted in the presence of NIL (*Online Supplementary Figure S1A*). TKI-persistent NF- $\kappa$ B activation was likewise evident *in vivo*, as shown by bone marrow (BM) immunohistochemical p65-staining of *Scl-tTa-BCR-ABL* or *Scl-tTa* control mice (Figure 1A). Although NIL slightly reduced p65 protein expression, reversion to healthy control levels was not achieved.

Next, we studied the effects, induced by pharmacologic inhibition of the I $\kappa$ B-kinase-subunit, IKK2 using LY. The small molecule inhibitor prevents IKK2-phosphorylation and subsequent degradation of I $\kappa$ B $\alpha$ , which thus remains bound to the NF- $\kappa$ B complex to block its phosphorylation. This prevents nuclear translocation of NF- $\kappa$ B and thereby expression of target genes. Analysis of *A20*-expression in human KCL22 CML-cells suggested a NIL-induced upregulation (Figure 1B, fc: 3.37), that was reduced by LY-treatment (*A20*, fc: 2.02). We observed similar effects when adding imatinib (IM) or dasatinib (DAS, *Online Supplementary Figure S1B*). We studied signaling activity via western blot analyses in KCL-22 cells (Figure 1C). As expected, phosphorylation of NF- $\kappa$ B subunit p65 was not reduced by NIL-treatment alone. Moreover, pI $\kappa$ B $\alpha$  at serine 32/36 was significantly inhibited by LY single-treatment (fc: 0.27) and this was still achieved in the presence of NIL (fc: 0.17), as shown by significant downregulation as compared to the corresponding DMSO control or

NIL-single treatment, in the presence of TNF. This further resulted in reduced phosphorylation of p65 at serine 536 in the presence of LY (fc: 0.42) or both drugs (fc: 0.29), as compared to the corresponding DMSO control.

AnnexinV-staining of treated KCL-22 cells showed the advantage of IKK $\beta$ -kinase inhibition as this induced a significant increase in apoptosis by IKK2-inhibition alone (fc: 2.4) that further enhanced NIL-induced cell death by 1.4-fold (Figure 1D). The therapeutic effect of IKK2-inhibition was also evaluated in the context of other clinically relevant TKIs. For all TKIs tested, we observed increased apoptosis levels upon combined treatment (DAS fc: 1.3, BOS fc: 1.4, PON fc: 1.3) (Figure 1D). We next treated isolated lin<sup>-</sup> bone marrow (BM) cells from *Scl-tTa-BCR-ABL* or *Scl-tTa* control mice (Figure 1E), showing that control cells remained largely unaffected whereas apoptosis was induced upon LY-monotherapy (fc: 2.2) in murine primary CML cells. Moreover, combined LY- and NIL-treatment enhanced NIL-induced apoptosis by 2.1-fold.

In order to study the role of TNF-signaling in BCR-ABL-kinase-mutated TKI-resistance, we utilized the KCL-22<sup>Y272H</sup>-<sup>9</sup> and KCL-22<sup>T315I</sup>-cell lines<sup>10</sup>. In KCL-22<sup>Y272H</sup> cells, LY-therapy induced apoptosis, while NIL alone had no effect (Figure 1F). As DAS, bosutinib (BOS), and ponatinib (PON) could bypass the P-loop mutation, these TKIs indeed induced KCL-22<sup>Y272H</sup> cell death that was further elevated with IKK2-inhibition, as reflected by a further rise in AnnexinV-positivity (DAS fc: 1.4, BOS fc: 1.3, PON fc: 1.5). In KCL-22<sup>T315I</sup> cells, effects were very modest with LY-application only slightly inducing apoptosis and this was unaffected by TKI-treatment (*Online Supplementary Figure S1C*).

To investigate whether IKK2-targeting could affect TKI-persistent LSCs, we implemented the *Scl-tTa-BCR-ABL* mouse model (Figure 2A). As expected, splenomegaly and white blood cell count (WBC) were normalized by NIL-treatment (*Online Supplementary Figure S2A+B*). Comprehensive immunophenotyping revealed a predominant expansion of malignant B-cells (B220<sup>low</sup>) that did respond to BCR-ABL-inhibition (*Online Supplementary Figure S2C+D*). Moreover, we confirmed our previous findings on reduced BM-derived long-term (LT)-HSCs (Lin<sup>-</sup>, Sca1<sup>+</sup>, c-kit<sup>+</sup>, CD48<sup>low</sup>, CD150<sup>+</sup>) upon disease development (Figure 2B).<sup>11</sup> In line with

the concept that TKI-treatment selects for primitive LSCs, we observed increased LT-HSCs in NIL- or NIL/LY-treated mice. Interestingly, LY-monotherapy decreased LT-HSCs by 2.3-fold. While *Tnf*-expression was decreased upon treatment in BM, NIL-monotherapy, as well as combined NIL/LY-therapy apparently increased *Tnf*-transcript levels in the spleen (Figure 2C). As TNF acts both, autocrine and paracrine, this likely resulted in elevated *A20*-expression in both organs (Figure 2C). In light of this, *A20* is not only described to be increased in response to TNF, but also known to protect cells from TNF-induced apoptosis.<sup>12</sup> Treatment efficacy was further shown by a reduction of *BCR-ABL*-expression, with the strongest reduction upon combined *BCR-ABL*- and *IKK2*-inhibition (Figure 2D). We assessed the malignant stem cell potential via serial transplantation of BM-cells into irradiated wt-recipients (Figure 2A). In line with our finding that BM-derived LT-HSCs are spared by TKI- or TKI+LY-treatment, secondary recipients showed disease recurrence, accompanied by slightly increased spleen weights (*Online Supplementary Figure S2E*), as well as elevated *BCR-ABL*-transcript levels (Figure 2E). Interestingly, LY-monotherapy prevented spleen expansion and severely impaired re-expansion of malignant cells as shown by only residual *BCR-ABL*-transcript levels, in secondary recipients.

To determine whether TNF-signaling is specifically active in LSCs, we reanalyzed microarray data (GSE40721) revealing upregulation of TNF-signaling via NF- $\kappa$ B in CD34<sup>+</sup>CD38<sup>-</sup>-stem- versus CD34<sup>+</sup>CD38<sup>+</sup>-progenitor cells (Figure 3A). We proceeded to evaluate the clonogenic potential in CML CD34<sup>+</sup>-cells upon treatment and this was strongly reduced by both single treatments, as compared to DMSO control (LY: 12.1-fold, NIL: 3.8-fold) and almost completely abrogated upon combined *IKK2* and *BCR-ABL*-targeting (77.5-fold, Figure 3B). To assess the effect on most primitive cells, replating was performed without any further treatment and this showed that previous NIL-treatment had spared malignant stem cells while LY-treated cells were severely impaired in the ability to form colonies (Figure 3C), suggesting that LY-monotherapy targets the most primitive malignant stem cells. In healthy-donor-derived CD34<sup>+</sup>-cells, *IKK2*-inhibition showed an effect in 2 out of 6 samples (*Online Supplementary Figure S3A*). As these cells were partially provided by osteoarthritis patients,

we assume that IKK2-inhibition could affect these samples, as pro-inflammatory cytokines could be likewise involved.<sup>13</sup> In order to dissect if IKK2-targeting induces apoptosis in the most primitive CML-cells we performed AnnexinV-staining in CD34<sup>+</sup>/CFSE<sup>MAX</sup> quiescent LSCs. Indeed, *in vitro* apoptosis was significantly increased by IKK2-inhibition alone (fc: 7.4) or in combination with NIL (fc: 8.5, Figure 3D), suggesting that LY-treatment exerts its anti-leukemic effects observed upon secondary transplantation at least partially by induction of apoptosis within the LSC-compartment.

As further LSC-persistence-mediating cytokines activate the NF- $\kappa$ B pathway, we next tested the treatment-effect in the presence of physiological IL-1 $\alpha$  or IL-1 $\beta$  levels (*Online Supplementary Figure S3B*). Again, colony formation was significantly reduced by inhibition of IKK2 alone (IL-1 $\alpha$ : 1.5-fold, IL-1 $\beta$ : 1.7-fold) as well as by combined IKK2- and BCR-ABL-targeting (IL-1 $\alpha$ : 3.4-fold, IL-1 $\beta$ : 5.2-fold), suggesting that IKK2-targeting could exerts its effects by inhibiting, not only TNF-mediated NF- $\kappa$ B activation but also due to targeting further pro-leukemic inflammatory signaling.

In the context of progressed disease, *IKK2* was described as a resistance-associated gene.<sup>14</sup> In line with this, TNF-signaling increased in BM CD34<sup>+</sup>-cells upon CML-progression (Figure 3E). Therefore, we studied IKK2-targeting also in primary BC-CML samples, showing that impaired colony formation was evident upon LY-exposure in all patient samples tested (CML-BC #1:10.9-fold; #2:7.4-fold; #3:13.9-fold, Figure 3F, *Online Supplementary Figure S3C*). Again, in combination this was further reduced by NIL (CML-BC #1:21.4-fold; #2:42-fold; #3:93.7-fold).

In conclusion, our results underline the potential of NF- $\kappa$ B-targeting via IKK2-inhibition, to eliminate LSCs, having the potential to re-expand upon TKI-discontinuation, which remain largely spared by NIL treatment. *In vivo* treatment revealed the complexity. While NIL alone and in combination was able to reduce leukemic cells, the LSCs persisted and reinitiated the disease upon secondary transplant. Treatment with NIL expanded CD3<sup>+</sup> T-cells, which was still observed when combined with LY but not in LY-monotherapy treated mice (*Online Supplementary Figure S2C*). As T-cells in CML display a TNF-dominated cytokine secretion

profile <sup>15</sup>, we assume this could be a source of enhanced splenic *Tnf*-expression, probably exerting paracrine effects on the BM, thereby potentially protecting BM-residing LSCs.

### **List of abbreviations**

BC: Blast crisis; BM: bone marrow; BOS: Bosutinib; CFU: Colony forming unit; CML: Chronic myeloid leukemia; CP: Chronic phase; DAS: Dasatinib; dtg: Double transgenic (SCLtTA/BCR-ABL); FBS: fetal bovine serum; GSEA: gene set enrichment analysis; h: human; HSC: Hematopoietic stem cell; LSC: leukemic stem cell; LSK: Lin<sup>-</sup>, Sca1<sup>+</sup>, ckit<sup>+</sup>; LT-HSC: Long-term hematopoietic stem cell (lin<sup>-</sup>, sca1<sup>+</sup>, ckit<sup>+</sup>, CD48<sup>low</sup>, CD150<sup>+</sup>); LY: LY2409881; m: murine; MNC: Mononucleated cell; NIL: Nilotinib; PB: peripheral blood; PON: Ponatinib; stg: Single transgenic (SCLtTA); TKI: Tyrosine kinase inhibitor; wt: wild type

## References

1. Giustacchini A, Thongjuea S, Barkas N, et al. Single-cell transcriptomics uncovers distinct molecular signatures of stem cells in chronic myeloid leukemia. *Nat Med*. 2017;23(6):692-702.
2. Herrmann O, Kuepper MKMK, Bütow M, et al. Infliximab therapy together with tyrosine kinase inhibition targets leukemic stem cells in chronic myeloid leukemia. *BMC Cancer*. 2019;19(658):1-14.
3. Hsieh MY, Van Etten RA. IKK-dependent activation of NF- $\kappa$ B contributes to myeloid and lymphoid leukemogenesis by BCR-ABL1. *Blood*. 2014;123(15):2401-2411.
4. Yamashita M, Passequé E. TNF- $\alpha$  Coordinates Hematopoietic Stem Cell Survival and Myeloid Regeneration. *Cell Stem Cell*. 2019;25(3):357-372.
5. Gallipoli P, Pellicano F, Morrison H, et al. Autocrine TNF- $\alpha$  production supports CML stem and progenitor cell survival and enhances their proliferation. *Blood*. 2013;122(19):3335-3339.
6. Sakurai H, Suzuki S, Kawasaki N, et al. Tumor necrosis factor- $\alpha$ -induced IKK phosphorylation of NF- $\kappa$ B p65 on serine 536 is mediated through the TRAF2, TRAF5, and TAK1 signaling pathway. *J Biol Chem*. 2003;278(38):36916-36923.
7. Brenner D, Blaser H, Mak TW. Regulation of tumour necrosis factor signalling: Live or let die. *Nat Rev Immunol*. 2015;15(6):362-374.
8. Deng C, Lipstein M, Rodriguez R, et al. The novel IKK2 inhibitor LY2409881 potently synergizes with histone deacetylase inhibitors in preclinical models of lymphoma through the downregulation of NF- $\kappa$ B. *Clin Cancer Res*. 2015;21(1):134-145.
9. Kuepper MKMK, Bütow M, Herrmann O, et al. Stem cell persistence in CML is mediated by extrinsically activated JAK1-STAT3 signaling. *Leukemia*. 2019;33(8):1964-1977.
10. Yuan H, Wang Z, Gao C, et al. BCR-ABL Gene Expression Is Required for Its Mutations in a Novel KCL-22 Cell Culture Model for Acquired Resistance of Chronic Myelogenous Leukemia. *J Biol Chem*. 2010;285(7):5085-5096.
11. Schemionek M, Elling C, Steidl U, et al. BCR-ABL enhances differentiation of long-term repopulating hematopoietic stem cells. *Blood*. 2010;115(16):3185-3195.
12. Priem D, Devos M, Druwé S, et al. A20 protects cells from TNF-induced apoptosis through linear ubiquitin-dependent and -independent mechanisms. *Cell Death Dis*. 2019;10(10):692.
13. Zhao Y, Li Y, Qu R, et al. Cortistatin binds to TNF- $\alpha$  receptors and protects against osteoarthritis. *EBioMedicine*. 2019;41:556-570.
14. Villuendas R, Steegmann JL, Pollán M, et al. Identification of genes involved in imatinib resistance in CML: A gene-expression profiling approach. *Leukemia*. 2006;20(6):1047-1054.
15. Westermann J, Van Lessen A, Schlimper C, et al. Simultaneous cytokine analysis by cytometric bead array for the detection of leukaemia-reactive T cells in patients with chronic myeloid leukaemia. *Br J*

Haematol. 2006;132(1):32-35.

## Figure Legends

### Figure 1: Targeting TKI-persistent TNF-signaling by pharmacological IKK2-inhibition.

**A** Elevated and TKI-persisting NF- $\kappa$ B-activation in CML mice is shown by a representative immunohistochemical bone marrow (BM) staining of NF- $\kappa$ B p65 (brown) and hematoxylin (blue) in BM sections from mice, which were either transplanted with *Scl-tTa-BCR-ABL* or *Scl-tTa* control BM and subsequently treated using nilotinib (NIL) or vehicle control for three weeks. White scale bar represents 50 $\mu$ m **B** CML KCL-22 cells were treated using LY (10 $\mu$ M), NIL (50nM), or LY + NIL, in the presence of 1ng/ml TNF for 16 h. Expression of *A20* was analyzed via qRT-PCR and is expressed as % of *GAPDH*. Shown are mean values of n=3, normalized to DMSO control. **C** Western blot analysis of KCL-22 cells using the indicated antibodies, pretreated with 1ng/ml TNF for 1h and subsequently treated using NIL (50nM) and/or LY (5 $\mu$ M) for again 1 h. Shown is one representative of n=3 (left panel). Phosphorylation was quantified using densitometry (n=3, right panel). Shown are means  $\pm$  SEM. **D** Flow cytometry analysis of AnnexinV-positive KCL-22 cells in the presence of 1ng/ml TNF after 48h of treatment using LY (5 $\mu$ M), NIL (50nM), LY + NIL, DAS (10nM), LY + DAS, BOS (5nM), LY + BOS, PON (5nM), LY + PON. **E** AnnexinV flow cytometry analysis of BM lin<sup>-</sup> MACS-isolated cells from *Scl-tTa* or *Scl-tTa-BCR-ABL* mice that were induced to express *BCR-ABL* for 10 days prior to BM-isolation. *In vitro* treatment was performed using LY (10 $\mu$ M), NIL (50nM), LY + NIL or DMSO control in the presence of 1ng/ml TNF for 16h (n=3). **F** Flow cytometry analysis of AnnexinV-positive KCL-22<sup>Y272H</sup> cells after 48h of treatment using LY (5 $\mu$ M), NIL (50 M), LY + NIL, DAS (10nM), LY + DAS, BOS (5nM), LY + BOS, PON (5nM), LY + PON in the presence of TNF (1ng/ml; n=3). Significances were calculated using one or two-way ANOVA; Mean  $\pm$  SD; \*p<0.05, \*\*p<0.01, \*\*\*p<0.001, \*\*\*\*p<0.0001

### Figure 2: IKK2-inhibition reduces LT-HSCs and inhibits disease reinitiation *in vivo*.

**A** Schematic overview of the experimental setup. 2x10<sup>6</sup> BM cells of either FVB/N *Scl-tTa* or *Scl-tTa-BCR-ABL* mice were transplanted into irradiated wt FVB/N recipients. Expression of *BCR-ABL* was induced one week after transplantation and treatment was started at two

weeks after transplant and continued for three weeks. During that time, LY was administered via intraperitoneal injection, three times per week (50mg/kg body weight, dissolved in 5% dextrose) and/or NIL-treatment was performed via oral gavage, daily (50mg/kg body weight, dissolved in 10% N-Methyl-2-pyrrolidone and 90% polyethylene glycol) and/or the corresponding vehicle control for 3 weeks daily. Following treatment groups were evaluated: *Scl-tTa* (vehicle, designated as control) or *Scl-tTa-BCR-ABL* (vehicle, LY, NIL, and LY+NIL). After sacrifice,  $2 \times 10^6$  BM-cells of treated animals were transplanted into secondary irradiated recipients. These mice were sacrificed for analyses 6 weeks after transplantation. **B** BM derived LT-HSCs ( $\text{lin}^-$ ,  $\text{Sca1}^+$ ,  $\text{ckit}^+$ ,  $\text{CD48}^{\text{low}}$ ,  $\text{CD150}^+$ ) of treated recipients, shown as % of living cells. **C** qRT-PCR analyses of *Tnf* and *A20* mRNA-expression in BM and spleen of treated primary recipients is shown relative to *Gapdh* [%]. **D** *BCR-ABL* mRNA-expression in BM of primary and secondary (**E**) recipients. Significances were calculated using one or two-way ANOVA; Mean  $\pm$  SD; \* $p < 0.05$ , \*\* $p < 0.01$ , \*\*\* $p < 0.001$ , \*\*\*\* $p < 0.0001$

**Figure 3: Targeting elevated NF- $\kappa$ B signaling substantially reduces CP- and BC-CML stem cells.**

**A** GSEA (Gene Set Enrichment Analysis) of published expression data set GSE40721 comparing CML- $\text{CD34}^+$ ;  $\text{CD38}^+$  progenitor- vs. CML- $\text{CD34}^+$ ;  $\text{CD38}^-$  stem-cells for the 'HALLMARK\_TNFA\_SIGNALING\_VIA\_NFKB' gene set. **B** CFU-assays using primary patient derived  $\text{CD34}^+$  BM-cells after being treated for 72h using LY (10 $\mu$ M), NIL (50nM), LY+NIL or DMSO control, in the presence of TNF (1ng/ml). **C** CFU-counts upon serial-plating using cells obtained in (B), without any further treatment. **D** Analysis of apoptotic and CFSE<sup>Max</sup>/AnnexinV  $\text{CD34}^+$  CML-CP patient derived BM-cells after being treated for 72h using LY (10 $\mu$ M), NIL (50nM), LY+NIL, or DMSO control, in the presence of TNF (1ng/ml). Shown is one out of three representative results. **E** GSEA of published expression data set GSE47927 comparing CML-CP HSCs vs. CML-BC HSCs analyzed for the 'HALLMARK\_TNFA\_SIGNALING\_VIA\_NFKB'-gene set. **F** CFU-assays of BC-CML-derived mononucleated (MNC) bone marrow cells being treated for 72h using LY (10 $\mu$ M), NIL

(50nM), LY+NIL, or DMSO control in the presence of TNF (1ng/ml). Significances were calculated using one or two-way ANOVA; Mean  $\pm$  SD; \*p<0.05, \*\*p<0.01, \*\*\*p<0.001, \*\*\*\*p<0.0001

Figure 1

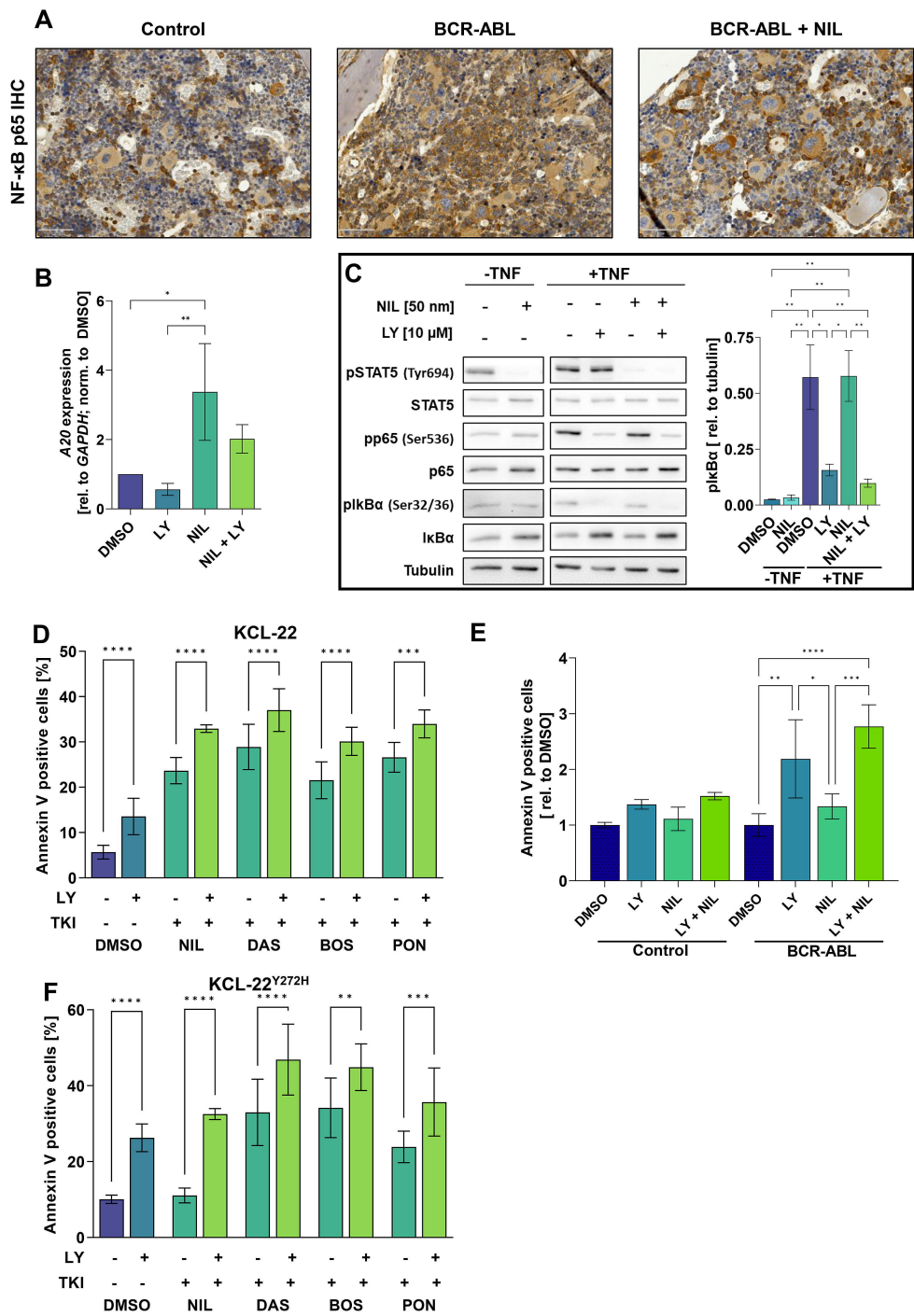
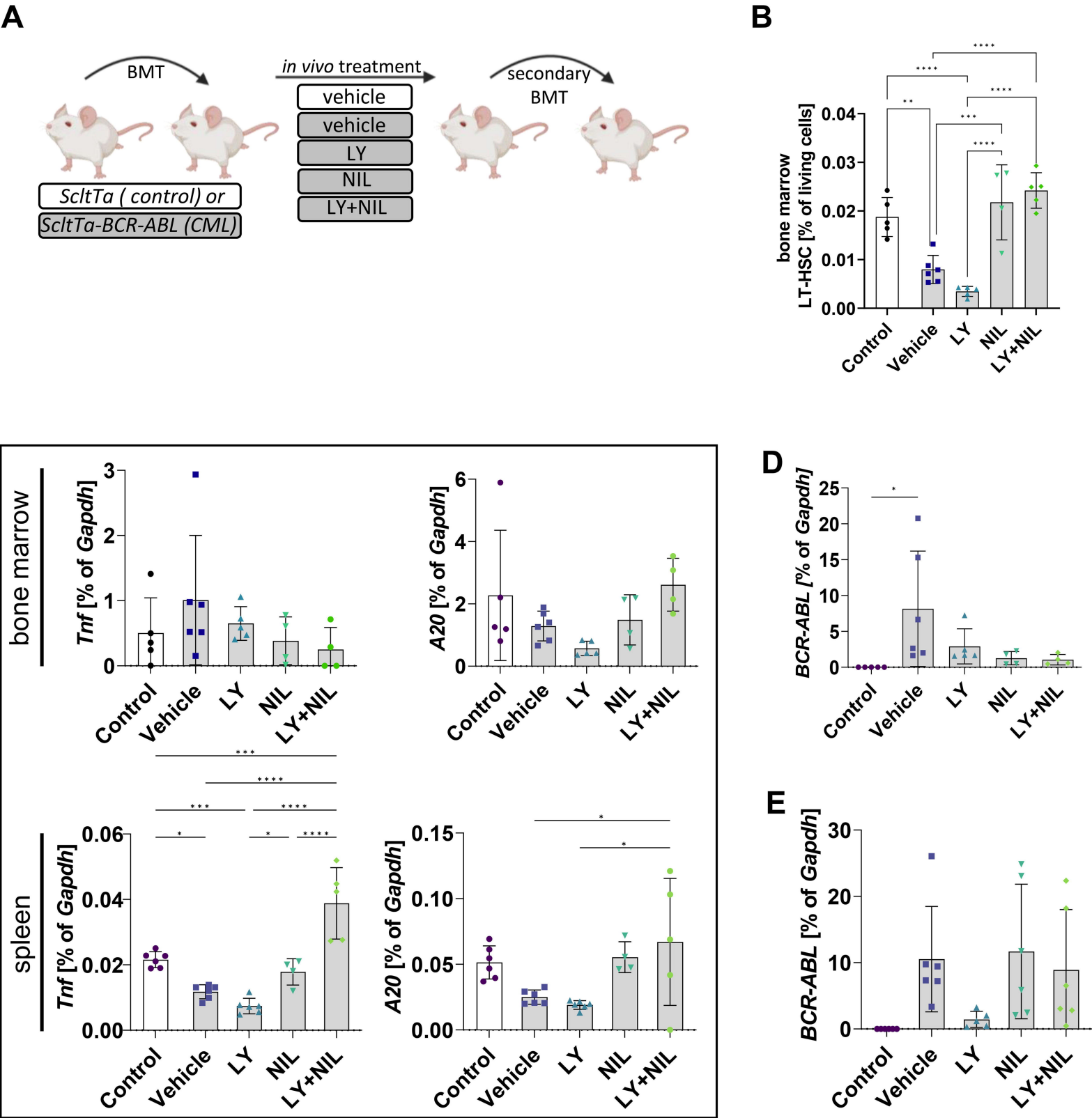
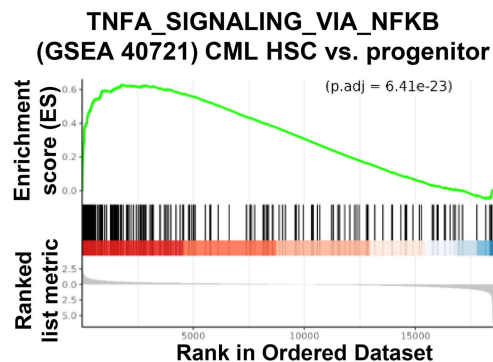


Figure 2

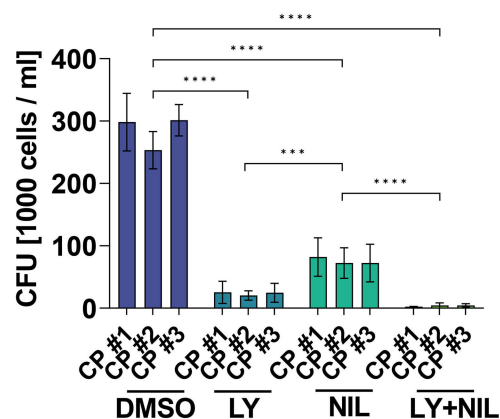


# Figure 3

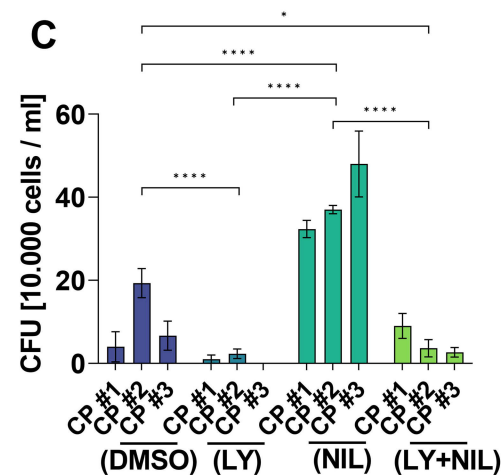
**A**



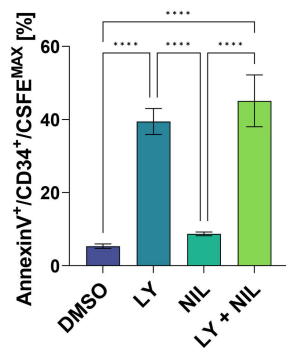
**B**



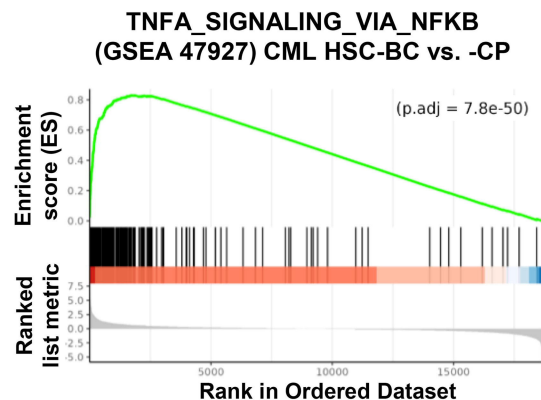
**C**



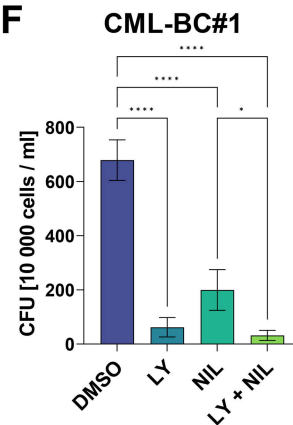
**D**



**E**



**F**



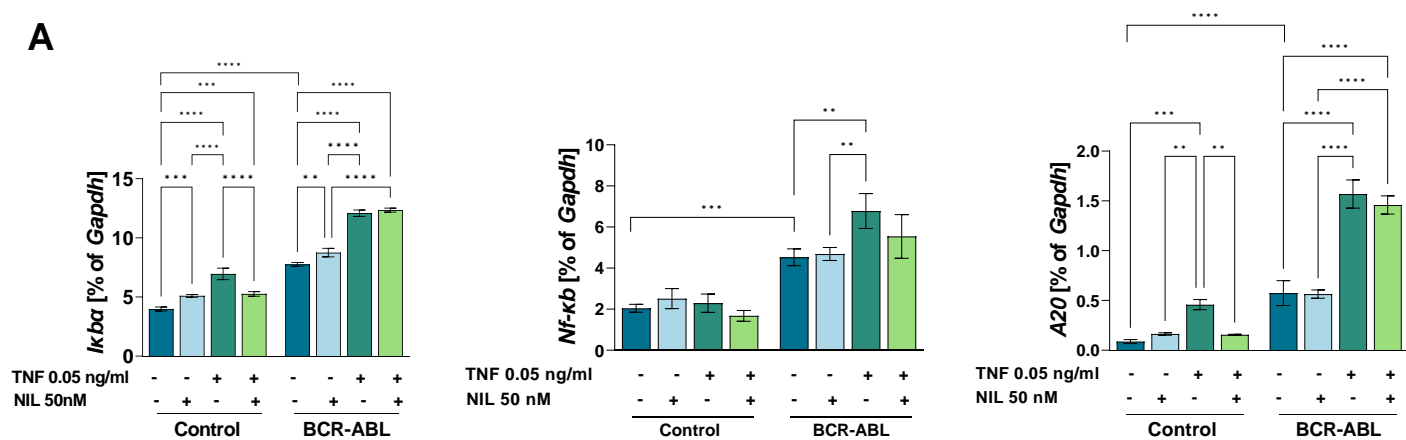
## Supplementary Appendix

# **Targeting cytokine-induced leukemic stem cell persistence in chronic myeloid leukemia by IKK2-inhibition**

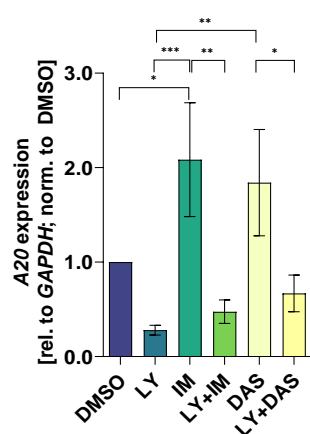
Marlena Bütow<sup>1,2</sup>, Fabio J. Testaquadra<sup>1,2</sup>, Julian Baumeister<sup>1,2</sup>, Tiago Maié<sup>3</sup>, Nicolas Chatain<sup>1,2</sup>, Timo Jaquet<sup>1,2</sup>, Stefan Tillmann<sup>1,2</sup>, Martina Crysandt<sup>1,2</sup>, Ivan G. Costa<sup>3</sup>, Tim H. Brümmendorf<sup>1,2</sup>, Mirle Schemionek<sup>1,2</sup>

<sup>1</sup>Department of Hematology, Oncology, Hemostaseology, and Stem Cell Transplantation, Faculty of Medicine, RWTH Aachen University, Aachen, Germany, <sup>2</sup>Center for Integrated Oncology Aachen Bonn Cologne Düsseldorf (CIO ABCD), Aachen, Germany, <sup>3</sup>Institute for Computational Genomics, Joint Research Center for Computational Biomedicine, RWTH Aachen University, Aachen, Germany

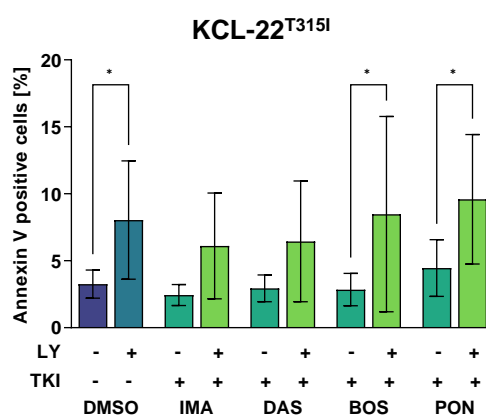
**A**



**B**

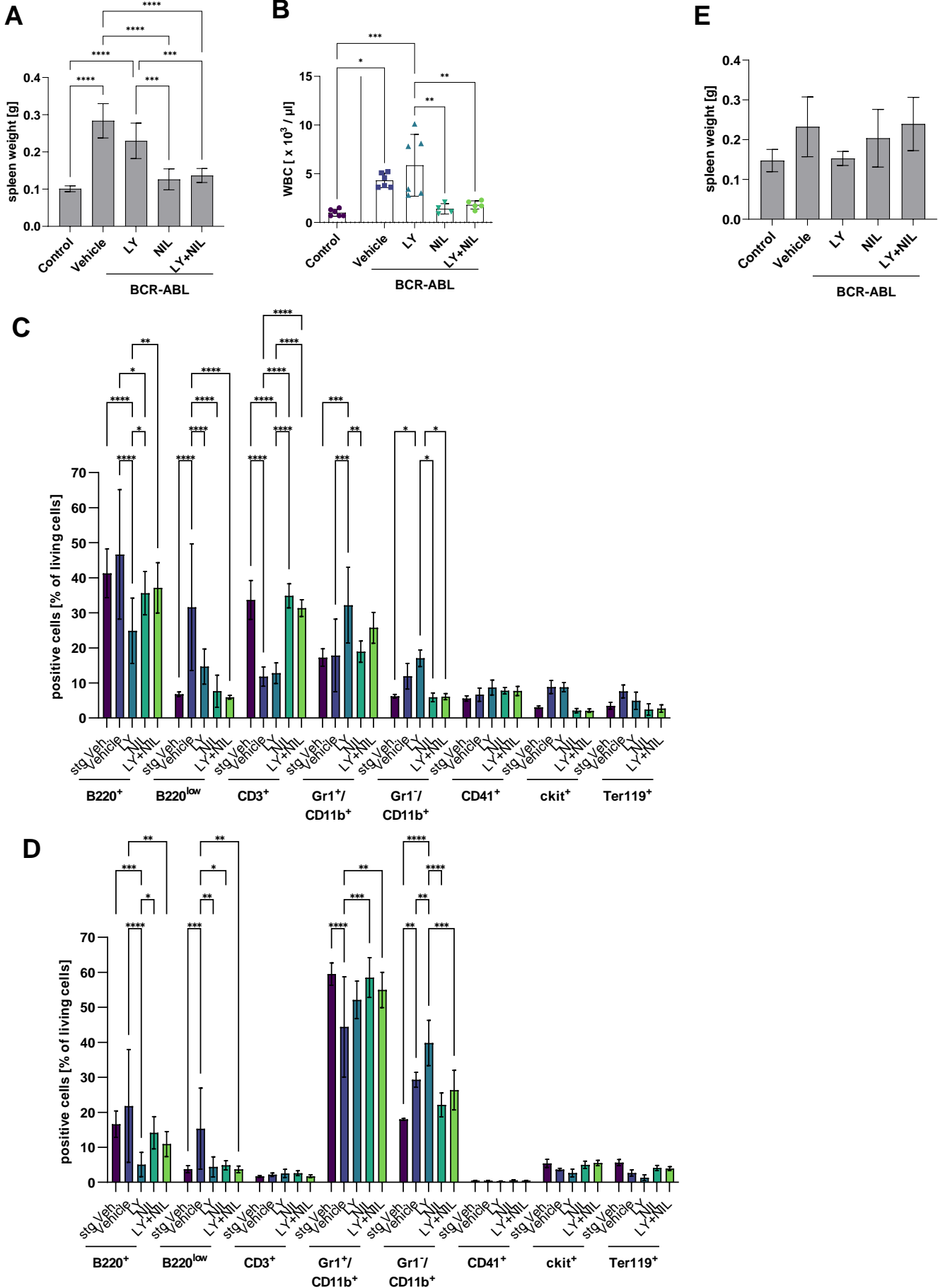


**C**

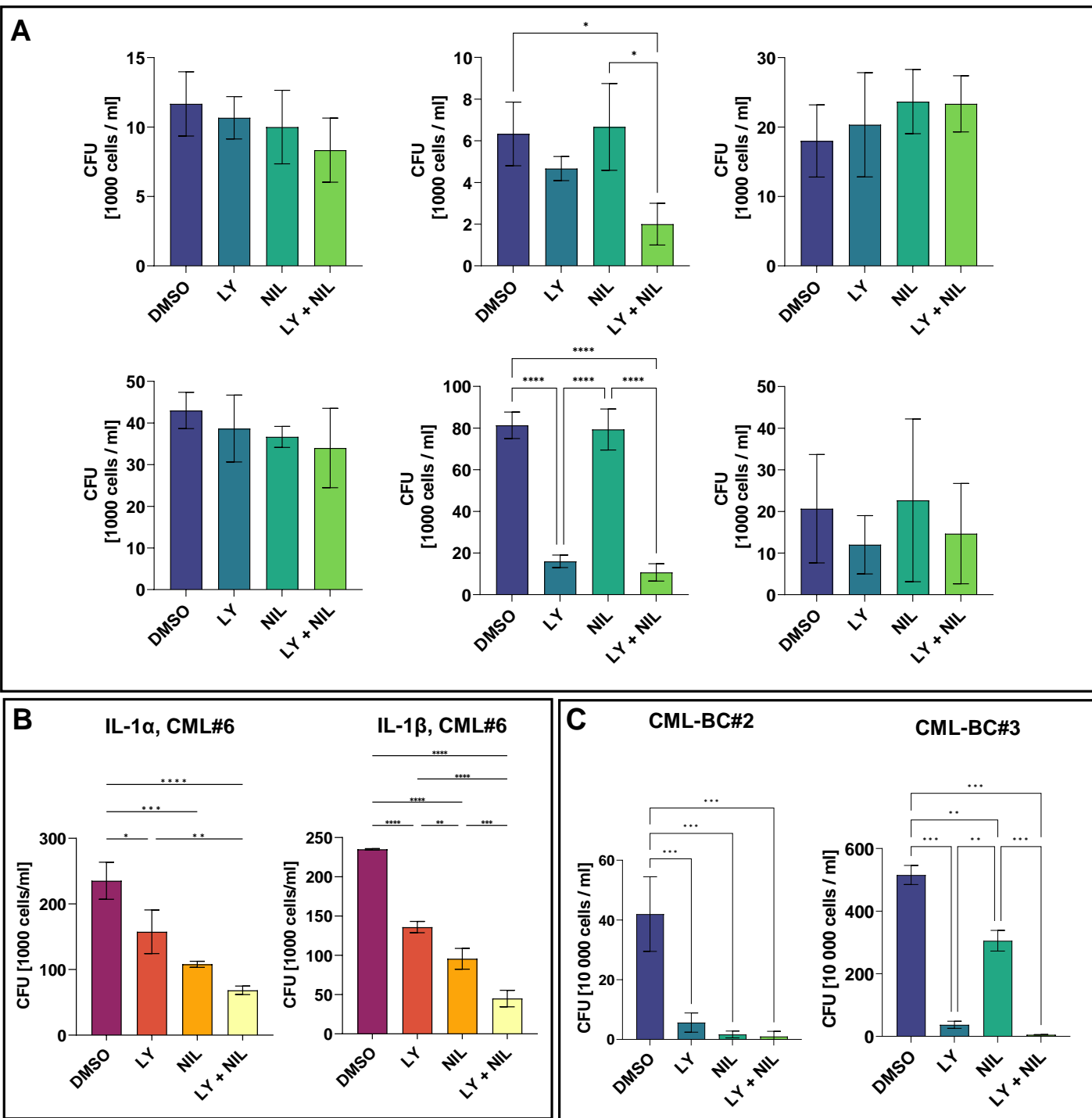


## Supplemental Figure S1

**S1A** Expression of *Ikba*, *NF-kB*, and *A20*-mRNA in BCR-ABL-negative control- and BCR-ABL-positive murine myeloid progenitor 32Dcl3 cells is shown as % of *Gapdh*. Cells were treated using 0.05 ng/ml TNF and/or 50 nM NIL for 30 min. One representative of n=3 is shown. **S1B** Human CML KCL-22 cells were treated using LY (10  $\mu$ M), IM (1  $\mu$ M), DAS (10 nM) or LY+IM, and LY+DAS, in the presence of 1 ng/ml TNF for 16h. Expression of *NF-kB*-target gene *A20* was analyzed via qRT-PCR. Shown are mean values of n=3, normalized to DMSO control. **S1C** Flow cytometry analyses of AnnexinV-positive KCL-22<sup>T315I</sup> cells upon 48h of treatment using LY (5  $\mu$ M), IM (1  $\mu$ M), LY+IM, DAS (10 nM), LY+DAS, BOS (5 nM), LY+BOS, PON (5 nM), LY+PON in the presence of TNF (1 ng/ml; n=3). Mean  $\pm$  SD, significances were calculated using one-way ANOVA. \*p<0.05, \*\*p<0.01, \*\*\*p<0.001, \*\*\*\*p<0.0001



**Supplemental Figure S2**  
**S1A** Spleen weight [g] upon final analysis of primary recipients, that were treated using the indicated drugs. **S1B** White blood cell count (WBC) upon final analysis. **S1C** FACS-positive cells in spleen and BM (**S1D**), shown as % of living cells for B-cells (B220<sup>+</sup>), immature B-cells (B220<sup>low</sup>), T-cells (CD3<sup>+</sup>), granulocytes (Gr1<sup>+</sup>/CD11b<sup>+</sup>), immature granulocytes (Gr1<sup>-</sup>/CD11b<sup>+</sup>), megakaryocytes (CD41<sup>+</sup>), ckit<sup>+</sup>-positive cells, and erythrocytes (Ter119<sup>+</sup>). **S1E** Spleen weight [g] upon final analysis of secondary recipients. Mean  $\pm$  SD, level of significance was calculated using one-way ANOVA. \*p<0.05, \*\*p<0.01, \*\*\*p<0.001, \*\*\*\*p<0.0001



### Supplemental Figure S3

**S3A** Healthy donor CD34+ cells were isolated from femoral heads and were treated for 72 h using LY (10  $\mu$ M), NIL (50 nM), LY+NIL, or DMSO control, in the presence of 1 ng/ml TNF. Subsequently, cells were seeded in methylcellulose and colonies were counted on day 10. **S3B** CFU-assays using CML-CP patient derived BM CD34+ cells after treatment using LY (10  $\mu$ M), NIL (50 nM), LY+NIL, or DMSO control, in the presence of IL-1 $\alpha$  (2.5 ng/ml, left panel) or IL-1 $\beta$  (3.5 ng/ml, right panel) for 72 h. One patient is presented as an example out of n=3. **S3C** CFU-assays of BC patient derived mononucleated BM being treated for 72 h using LY (10  $\mu$ M), NIL (50 nM), LY+NIL, or DMSO control, in the presence of TNF (1 ng/ml). Mean  $\pm$  SD, level of significance was calculated using one-way ANOVA. \*p<0.05, \*\*p<0.01, \*\*\*p<0.001, \*\*\*\*p<0.0001